Development of a cascaded fine pointing and tracking control loop for quantum key distribution via free-space optical communications

René Rüddenklau[a], Eltimir Peev[a], and Florian Moll[a]

[a]German Aerospace Center (DLR e.V.), Institute of Communications and Navigation, Optical Satellite Links, Münchenerstraße 20, 82234 Oberpfaffenhofen, Germany

ABSTRACT

Satellite based quantum key distribution (QKD) enables the delivery of keys for quantum secure communications over long distances. Maturity of the technology as well as industrial interest are ever increasing. Same is true for satellite free-space optical communications (FSOC). In order to enable a robust channel for transmission it is indispensable to account for static and dynamically changing misalignments between the transmitter and receiver pair. This work will focus on the transmitter terminal (Alice) and the design and verification process of the active beam steering system. The novelty is a recently developed variable reluctance fine steering mirror (FSM) including eddy current sensors (ECS) to measure its tip and tilt. A cascaded architecture was chosen in order to combine the optical stabilization objective with the dynamics of the mirror platform. The inner control loop makes use of an observer model whose estimated output is fed into a state controller allowing for an increased responsiveness. While high gains increase the closed loop bandwidth the eigenfrequency of the system introduces a pole to the plant which has to be avoided by the controller output. A digital notch filter was introduced to reject the excitation of the critical frequency band which gets obsolete in a system with high frequency sampling capabilities. The outer loop is engaged when a valid optical signal is received and a transition from a closed loop pointing to a closed loop tracking mode is performed. A proportional-integral (PI) controller keeps the received beam at the 4-quadrant-diode (4QD) whose center is used as the main reference through prior calibration with the transmit beam launching on the same path. The presented cascaded control scheme allows improvements in system performance and reliability.

Keywords: free-space optical communications, tracking, fine pointing, cascaded control loop, fine steering mirror, quantum key distribution

1. INTRODUCTION

FSOC is already well established for transmitting high-speed and long-range data. It is also being extended further and further into space, either for high-speed optical downlinks to transmit data generated on a satellite or as a network node to relay data. Optical links may also provide an infrastructure for future secure communications with QKD. Experiments on the ground with fiber optic links have been widely used to demonstrate this technology and also to show the limitation of transmission range due to attenuation in optical fibers. Therefore, free space links can help to overcome this limitation by using satellite-based terminals for long distances, as in the optical space infrared downlink system (OSIRIS)[1] program. DLR's OSIRISv3[2] terminal payload provides a base that can be modified to serve as a terminal for multiple QKD sources in addition to the already integrated classical communications system. Said terminal was used to integrate the necessary elements to demonstrate a quantum-secure ground-to-ground link in an engineering demonstration over a 300 m link. In order to come as close as possible to a system that can also be used in satellite missions, a prototype FSM developed by Demcon and explicitly designed for space applications was evaluated.[3]

Further author information:
René Rüddenklau: e-mail: rene.rueddenklau@dlr.de, telephone: +49 (0)815328 2825

1.1 QuNET-alpha

The system was investigated experimentally in a field test as part of the German QuNET initiative* which addresses the use case of quantum secure communications for public authorities. The results of the experiment are used to model a feasible LEO satellite-ground link. Performance indicators such as quantum bit error rate and secure key rates of a potential mission can be estimated analytically. The transmission direction of the quantum channel originates from Alice to Bob which would also be the downlink channel in the case of a direct-to-earth (DTE) scenario. This work focusses on the Alice terminal.

1.2 Alice Terminal

In the satellite QKD scenario, the Alice terminal would be the transmitter terminal in a DTE downlink. It is responsible for sending the quantum and synchronization signals for the QKD systems, the data signal for the public channel, the beacon signal signal for the pointing, acquisition and tracking (PAT) of the Bob system, and an auxiliary signal for channel measurements and monitoring. The optical system of the Alice terminal (see Fig. 1)** consists of a compression telescope with a magnification of about two, followed by an aperture with a diameter of 11.3 mm. The received and transmitted signals both get reflected on the FSM, which is actively controlled to keep the beam on the receiver front end (RFE) by minimizing the error on the 4QD. A beam splitter (DCM2) is used to split the beam into the classical data signal (1604.88 nm) and the tracking beacon (1589.57 nm). Another beam splitter (DCM1) couples the transmitted classical and quantum signals into the actively controlled path. The transmit and receive paths are aligned before operation.

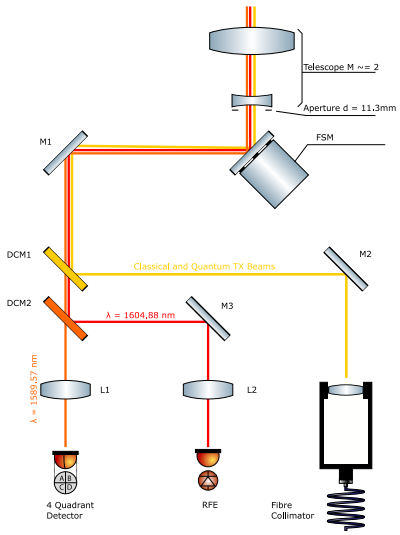

Figure 1. The design of the optical system inherited from OSIRISv3 including the FSM actuator and the 4QD sensor mandatory for optical tracking purposes.

2. SYSTEM CHARACTERIZATION

In order to use the terminal for a FSOC, a dedicated set of sensors and actuators must be operated in closed loop configuration. The optical sensor of the tracking loop is a 4QD, which is aligned with the RFE and therefore allows to detect any variations of the angle of incidence (AOI) which would minimize the power of the data

*https://www.qunet-initiative.de/
**graphics library: http://www.gwoptics.org/ComponentLibrary/

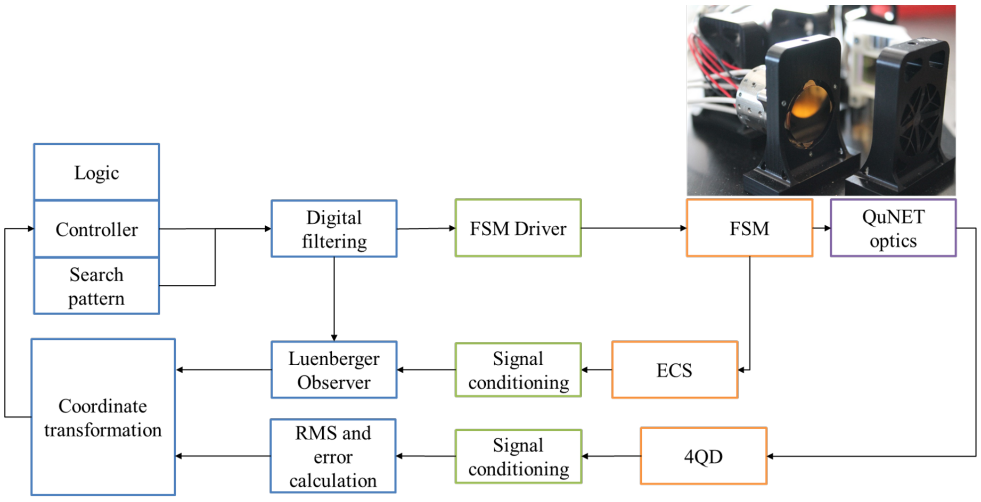

Figure 2. Cascaded control scheme which was developed during the QuNET-alpha project to account for the two individual optical and mechanical plants.

signal. A FSM is used to compensate for these angular variations within the system to ensure robust data reception in the receive path and stabilized transmission of the classical and quantum data signals. The FSM itself contains a proprietary feedback system with ECS from Kaman to measure the distance to the mirror platform, which can be post-processed to a mechanical angle. This is an advantageous feature because it allows the mirror to be controlled in a separate position control loop, enabling precise closed-loop pointing even in the absence of optical feedback. In addition, the mechanical jitter caused by micro-vibration can be suppressed independently of the bandwidth requirements for the optical control loop. The entire control system consists of various subcomponents (see Fig. 2) in the optical (purple), mechanical (orange), and electronic (green) domains. An ATSAMV71 microcontroller from Microchip was used to execute the control logic (blue), to drive the custom electronics, to provide telemetry, and to accept commands via a user interface. Since the tracking beacon is modulated by a 10 kHz signal to distinguish it from the background light, a second microcontroller was used to perform a root-mean-square (RMS) algorithm at 21 kHz and a position error calculation to provide real-time information to the main device. It was discovered that the sampling, and any time delay that can occur between the read out of individuals quadrants, is of paramount importance and should therefore be performed simultaneously for optimal performance. More specifically, to avoid scintillation effects within a single iteration that may otherwise result in inaccurate position readings. The configuration uses the 4QD feedback as the outer loop and the additional feedback from the ECS as the inner loop to build a cascaded control scheme. To evaluate the responsiveness of the overall system, the individual actuators and sensors were characterized in advance.

2.1 Optical feedback system

The 4QD is the main reference source of the optical terminal. It was selected for its good signal-to-noise ratio (SNR) and its ability to accurately determine the center position. A drawback of this sensor is the nonlinear error function of the calculated normalized position with respect to an external reference coordinate system. As shown in Fig. 4, the response curve drops after reaching the maximum value, indicating an additional non-bijective relationship from normed to absolute coordinates. To obtain a representative model for the simulation, a physical optics propagation (POP) was generated with Zemax to model the theoretical spot shape of the incoming beam at the 4QD sensor. The plane itself is at a slightly defocused distance to prevent a focused beam from disappearing in the non-active gaps between quadrants. The plotted response curves can be calculated using the euclidean norm

$$| \vec{qd}_{pos}(x,y) | = \sqrt{qd_{x-pos}(x,y)^2 + qd_{y-pos}(x,y)^2} \tag{1}$$

of the power normalized 4QD position errors as a function of the x-coordinate $qd_{x-plane}$ and the y-coordinate $qd_{y-plane}$ reference coordinates at the 4QD plane. The processed data were used to evaluate the expected

feedback sensitivity of the sensor and to determine whether the overall spot shape involves mutual coupling between the AOI and the error function. As shown in Fig. 3, there is no significant change in the slope and shape of the feedback curve over the variation of the AOI. Therefore, the optical feedback in this system can be considered as a single-input single-output (SISO) system. Note that in all cases a unique center position, with the error value equalling zero, can be found.

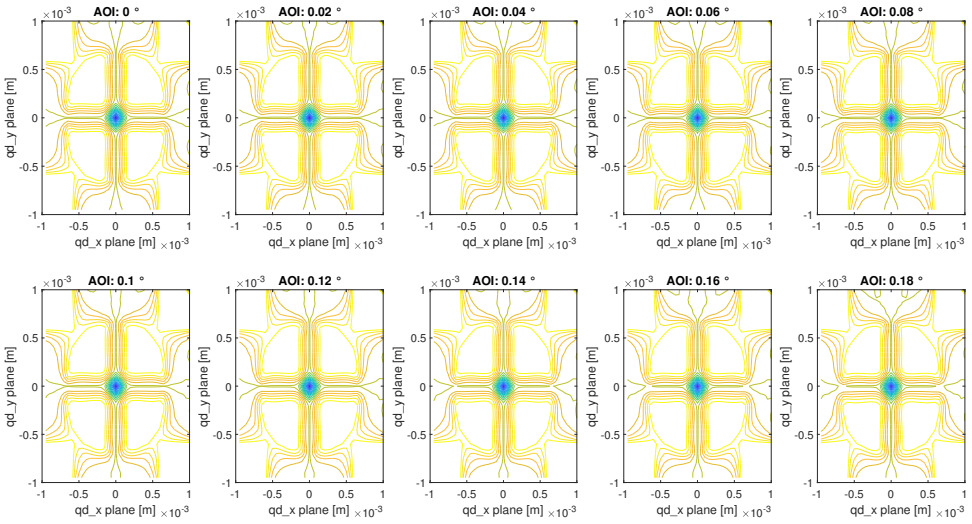

Figure 3. Variation of the AOI for simulated 4QD response data.

The built system contains a FSM whose actuator axes are rotated by 45° with respect to the 4QD coordinate systems for reasons of mechanical integration. As a result, a coordinate transformation must be performed to match the measured error. Figure 4 is plotted with respect to the FSM axes and shows the diagonally oriented error function of the detector.

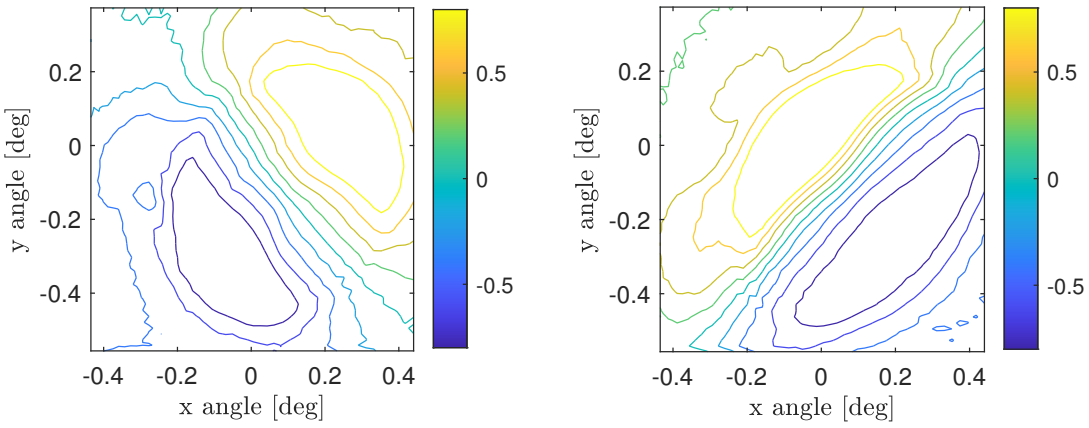

Figure 4. The optical position errors qd_{x-pos} (a) and qd_{y-pos} (b) as a function of the FSM angle are displayed. Parallel contour lines indicate the linear gain region towards the center of the detector.

2.2 Fine pointing assembly

The fine pointing assembly (FPA) contains a FSM and a set of ECS. The actuators of the FSM are driven by variable reluctance and can therefore be operated bidirectional in contrary to an ordinary solenoid. The moving platform is supported by a flexure acting as a spring and therefore introduces a pair of complex poles into the dynamic system, ultimately leading to the ability to oscillate. It results in a first eigenfrequency of about 120 Hz. If the output signal is left unprocessed, overshoot of the desired angular excitation will occur and may cause the mechanical end stops are hit at large strokes, which should be avoided to reduce degradation. Another effect is magnetic hysteresis caused by the actuator design principle. To verify the full range, hysteresis effects and to correlate axis orientation the actuator is driven in open loop configuration as seen in Fig. 5.

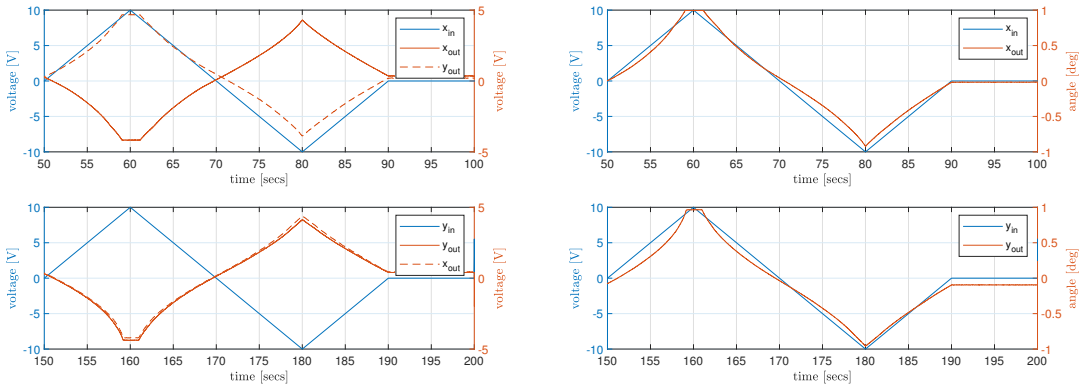

(a) (b)

Figure 5. Raw voltage readings from the sensors (a) and converted angles (b).

3. CONTROL LOOP DEVELOPMENT

The baseline is developed in a simulated environment, as it allows access to many parameters that are often either impossible or expensive to measure on the real hardware. Another valuable advantage is that this model can be developed independently, even simultaneously with the corresponding system. The following section describes the different elements of the control system and their structure. Figure 6 gives an overview of the architecture. Due to the limited computational resources in the developed highly integrated system, an inner loop sampling rate of 2 kHz was achieved as an upper limit. Closed-loop bandwidth improvements can be achieved with higher sampling rates, as shown in section 4.2. The general idea is to use a state controller for the FSM to decouple its dynamics from the disturbances that occur in the optical systems above (see section 3.4). To obtain information about the two states per mirror axis, a Luenberger observer was implemented to estimate the angular velocity. This avoids obtaining the derivative of a measured, noisy signal (see 3.3 section). To obtain a steady-state error of zero in pointing mode, a temporary integral controller is added to the output. To exclude the excitation of the natural oscillation frequency of the mirror platform, a digital notch filter processes the desired signals before they are sent to the driver (see section 3.2).

3.1 Optical loop

The optical tracking loop requirements are met by a proportional-integral controller that receives feedback from the processed position errors of the 4QD and passes the calculated control value to the FSM driver. This loop is automatically activated when the sum value of the quadrants exceeds a well-defined threshold. Minimizing the optical error signal is the primary goal to enable data transmission. If beacon tracking is lost, the internal state machine automatically reverts to a spiral search pattern in closed-loop scan mode until a new, valid signal is received.

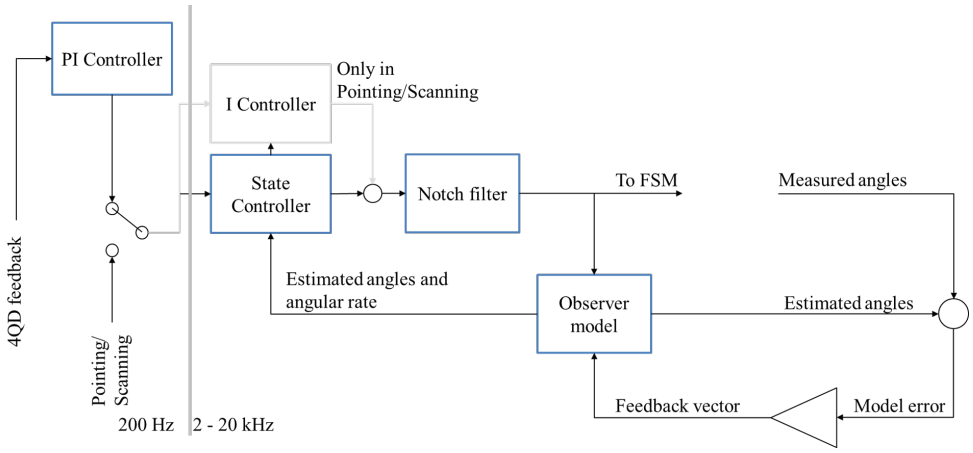

Figure 6. Control loop architecture which includes an outer loop at 200 Hz sampling frequency and an inner loop at 2kHz up to 20 kHz dependent on the processing capabilities.

3.2 Digital filtering

As mentioned in section 2.2, the mirror platform resonates at a frequency close to the control bandwidth. Unintended excitation at this frequency will destabilize the control loop and, in the worst case, cause loss of tracking. One way to mitigate the intrinsic response at a given frequency is a notch filter. The filter design for the specific unit was calculated with a center frequency of 118.5 Hz and a suppression bandwidth of 20 $\frac{\text{rad}}{\text{s}}$. The Tustin transformation was then used to transfer this filter into a discrete system with a sampling frequency of 2 kHz. This method is preferred over others because it provides accurate frequency matching between continuous and discrete time domains. Small shifts in the design frequency may occur, but are eliminated by pre-warping the continuous transfer function and was realized with a biquad filter implementation. The retrieved filter transfer function is

$$G_{nf}(z) = \frac{0.9951z^2 - 1.854z + 0.9951}{z^2 - 1.854z + 0.9903}. \tag{2}$$

Figure 7 validates the suppression of the oscillating behaviour in comparison with the natural response to a step function.

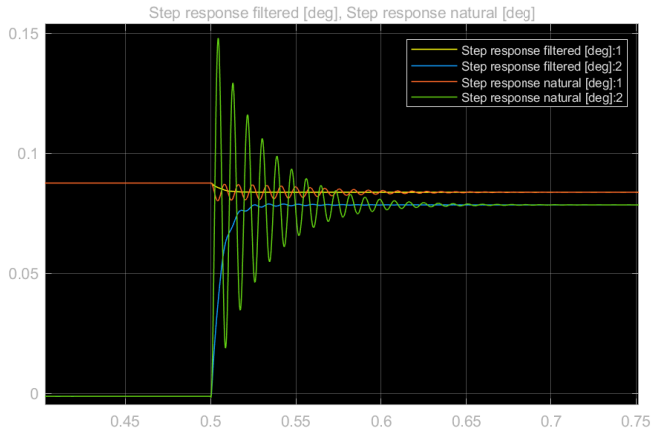

Figure 7. Notch filter performance in comparison to the natural transfer function of the FSM with angles in degrees and time axis in seconds.

3.3 Observer state estimation

The envisaged controller uses the angular excitation and rotation rate states as feedback. Its implementation, called state controller, is explained in the following section 3.4. The remaining state must be estimated by an observer, since only the angle of the FSM can be measured directly. This is possible due to the observability of the system, which can be validated by the system matrix A and the output matrix C of the state space representation. For this purpose, a Luenberger observer implementation was chosen in accordance with deterministic system dynamics. The internal model is run in parallel with the control loop. The desired bandwidth of the internal model can be set by tuning the observer gains using the pole placement method. While this approach increases the computational load on the processor, it can also be used to smooth the original measured position signal. Two implementations were considered for the internal model. The first represents a theoretical second-order system with $\omega_0 = 118.5\text{Hz}$ and $\zeta = 0.0190$ and is a SISO system, as shown in Eq. (3). The second, more sophisticated approach, as seen in Eqs. (4) and (5), uses the transfer function model determined by ECS measurements, which also accounts for cross-coupling and sensor-actuator rotation, and thus should be considered as multi-input multi-output (MIMO).

$$G_{mod}(s) = \frac{5.544 \cdot 10^5}{s^2 + 28.29s + 5.544 \cdot 10^5} \frac{deg}{deg} \tag{3}$$

$$G_{meas_{x\to x}}(s) = \frac{131.5s - 1.666 \cdot 10^6}{s^2 + 28.38s + 5.893 \cdot 10^5} \frac{V}{V} \quad G_{meas_{x\to y}}(s) = \frac{-93.99s + 1.788 \cdot 10^6}{s^2 + 19.93s + 6.063 \cdot 10^5} \frac{V}{V} \tag{4}$$

$$G_{meas_{y\to y}}(s) = \frac{338.2s - 1.808 \cdot 10^6}{s^2 + 20.94s + 5.818 \cdot 10^5} \frac{V}{V} \quad G_{meas_{y\to x}}(s) = \frac{180.8s - 1.702 \cdot 10^6}{s^2 + 28s + 5.927 \cdot 10^5} \frac{V}{V} \tag{5}$$

As expected, the MIMO model shows more accurate open loop results in comparison with the measurement reference data than the SISO system. Unlike the SISO model, there is no need to perform coordinate transformations before comparing to the measured output. However, the resulting state vector needs to be rotated into the actuator's coordinate system eventually to apply it to the correct axis. Due to reasonable performance of the SISO approach in closed-loop operation, it was chosen for the Alice terminal application to optimize processing overhead.

3.4 State controller design

Considering that the FSM loop must run at least an order of magnitude faster than the outer optical loop, a responsive controller design must be achieved. A common method for determining the gain of a state controller is to set the poles of the closed-loop response to a desired frequency. However, this does not take into account how much effort is required to achieve this goal. Likewise, it is not specified how well the individual errors of the states should be compensated. Following the idea that the inner loop acts as a cost minimizer for the master controller, an optimal control approach seems to be the best choice. To speed up the process of finding the appropriate parameters, the linear quadratic regulator (LQR) can be used to minimize the cost function

$$J(u) = \int (x^T Q x + u^T R u + 2x^T N u) dt \tag{6}$$

for a linear system $\dot{x} = Ax + Bu$ with the state-feedback being $u = -Kx$ where K is the desired gain vector. Since the state-space representation of the control loop is already known due to the model-based realization of the observer, the solution is straight forward. The integral controller can then be adjusted to minimize the error in the steady state response. Regardless of the current state of the outer tracking loop, the inner loop involving the ECS and the FSM itself runs continuously. Either in fixed pointing mode, or when performing a search pattern. Additionally to support the optical loop by taking the dynamic behaviour of the FSM during any vibration induced by external sources into account.

4. HARDWARE IMPLEMENTATION

After characterizing the system and developing a control architecture, as well as designing the controllers themselves, it was necessary to implement and optimize the critical parameters to fit a real-world environment.

4.1 Demonstration campaign setup

This development was part of a demonstration campaign between two public authorities in Bonn, Germany. For this purpose, a system was built[4] incorporating the previously discussed controls to establish a 300 m quantum-secure link. Figure 8 shows the resulting error in normalized 4QD space, which has an absolute range of [0;1]. It can be seen that the closed loop performs better than the optical open loop up to a frequency of 30 Hz. After this frequency, a transition occurs at about 40 Hz. This is due to the fact that higher bandwidth controllers can pick up high frequency noise and therefore start to correct for it, while slower controllers would act as low pass filters in this case. In this scenario, the performance of the tracking system was sufficient at all times to

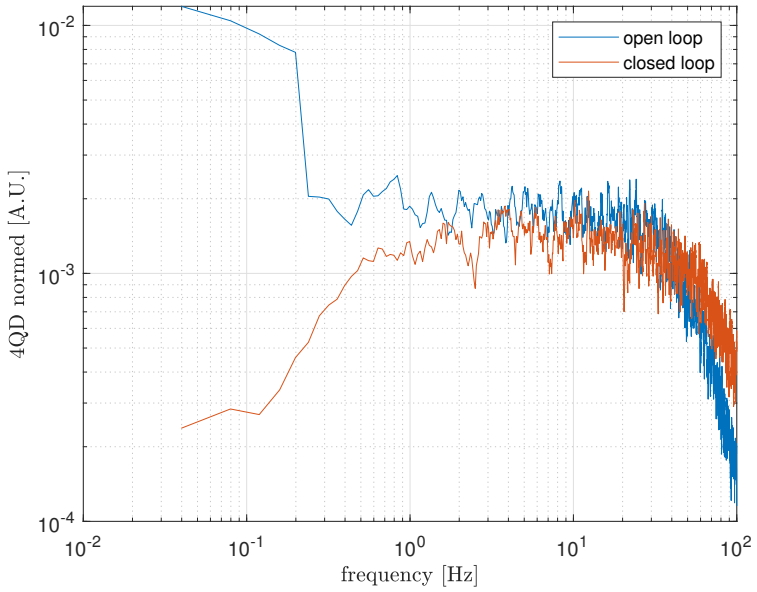

Figure 8. Measured fast fourier transform (FFT) at the Bonn campaign 2021 for free-space QKD demonstration.

establish a stable connection to the Bob terminal. However, it also became clear that the bandwidth of the optical control loop reaches its limits, especially with low beacon power and thus reduced SNR. Specifically in the case studied, higher frequency interference was caused by people passing by and vibrations in the building, which were introduced into the FSM mechanism itself and not into the optical path, where they would only show up as a secondary effect. This is another reason why the disturbances discussed should be handled in a decoupled manner by a dedicated and optimized FSM control loop. Further improvements and advantages will be shown in the following section.

4.2 Performance improvements using cascaded control

A real-time capable system was set up to perform hardware-in-the-loop (HIL) tests with the FSM in stand-alone configuration to verify performance at high sampling frequencies. Figure 9 was recorded using the same controller architecture as described previously, but with a sampling frequency of 20 kHz and fine tuned controller gains that were found to be $K_{position} = 19 \cdot 10^4 \ \frac{\text{int16\_t}}{\text{deg}}$, $K_{velocity} = 200 \ \frac{\text{int16\_t}}{\text{deg}}$, and $I = 45 \cdot 10^6 \ \frac{\text{int16\_t}}{\text{deg}}$. Compared to the uncontrolled step response, a more than ten times faster settling time with suppression of the oscillatory response was achieved without the need of an additional notch filter. This becomes possible as a result of higher bandwidths compared to the frequency band of the natural frequency. A small amount of cross-coupling can be seen, which may be due to the design of the actuator itself or to a mounting misalignment that results in an angular displacement between the actuator and sensors which deviates slightly from the assumed 45°. It can be eliminated by calibrating the system with respect to a fixed optical reference, such as a position sensitive device (PSD).

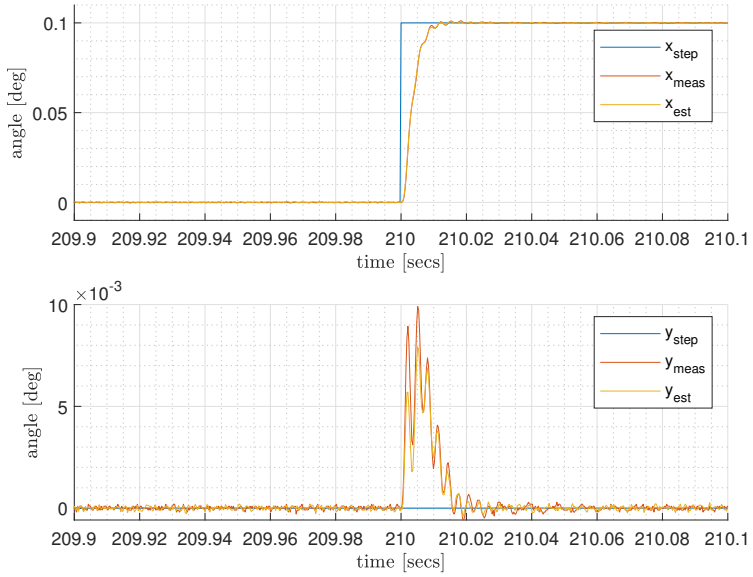

Figure 9. Closed loop step response with active state controller operated within a HiL test bench. That includes the electronics driver, the FSM actuator, the ECS and its corresponding readout electronics.

Another benefit of this cascaded control is the minimization of lag error when following the desired trajectory of a search pattern. It is important that the path is tracked accurately so as not to unintentionally miss the tracking beacon, thus maximizing system uptime. The open-loop and closed-loop performance is contrasted in Fig. 10. On one hand in passive operation, effects such as hysteresis and inertia can be seen. On the other hand, only marginal delays are expected in the active control case, hence being the preferred solution. Remaining known offsets can be reduced even further by feed forwarding them to the FSM driver.

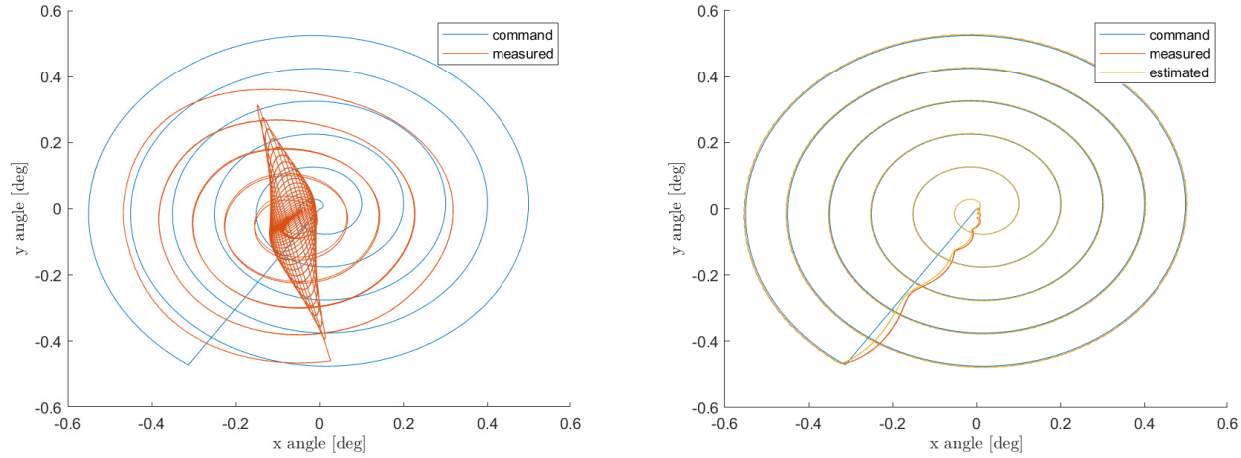

Figure 10. Commanded spiral trajectory with superimposed measured signal in open loop (a) and closed loop (b) operation.

5. CONCLUSION AND OUTLOOK

It has been demonstrated that a newly developed FSM for space applications can be used for FSOC applications. The design of the mirror can achieve high bandwidths and cover an optical scanning area of $\pm 2^{\circ}$. However, side effects such as hysteresis and natural resonant frequencies do occur. These can be overcome by introducing an adapted control loop with angular sensors, as shown in this work. Another advantage of this approach is that high-frequency, mechanically induced noise can be suppressed before it interferes with the overlying optical tracking loop. This development and other improvements will be used in upcoming satellite missions. A new challenge here will be the space environment in general and expected stronger micro-vibrations that place high demands on the FSM control loop. In addition, a coarse pointing assembly (CPA) will be mounted in front of the optical systems to provide platform-independent beam control. The FPA and CPA can be extended to work together by using the accurate position information provided by the 4QD and the resulting offsets measured by the ECS inside the FSM. By offloading these angles to the CPA and thus desaturating the limited range of the FPA, slow-moving attitude errors will be separated from fast-moving jitter.

ACKNOWLEDGMENTS

The project on which this report is based was funded by the German Federal Ministry of Education and Research under the funding code 16KIS1079. The author is responsible for the content of this publication.

REFERENCES

[1] C. Menninger, F. Moll, and B. Rödiger, "Dual wavelength optical system for multiple quantum communication transmitters in Cubesat platform," in *International Conference on Space Optics — ICSO 2020*, B. Cugny, Z. Sodnik, and N. Karafolas, eds., **11852**, p. 118525M, International Society for Optics and Photonics, SPIE, 2021.

[2] C. Fuchs and C. Schmidt, "Update on DLR's OSIRIS program," in *International Conference on Space Optics — ICSO 2018*, Z. Sodnik, N. Karafolas, and B. Cugny, eds., **11180**, p. 111800I, International Society for Optics and Photonics, SPIE, 2019.

[3] G. Witvoet, S. Kuiper, and A. Meskers, "Performance validation of a high-bandwidth fine steering mirror for optical communications," in *International Conference on Space Optics — ICSO 2018*, Z. Sodnik, N. Karafolas, and B. Cugny, eds., **11180**, p. 1118061, International Society for Optics and Photonics, SPIE, 2019.

[4] F. Moll, J. Krause, N. Walenta, R. Freund, E. Peev, A. Reeves, R. Rüddenklau, A. Ferenczi, L. Macri, S. Häusler, J. P. Labrador, M.-T. Hahn, J. Poliak, D. Orsucci, and F. Fohlmeister, "Link technology for all-optical satellite-based quantum key distribution system in c-/l-band," in *2022 IEEE International Conference on Space Optical Systems and Applications (ICSOS)*, pp. 275–280, 2022.